Measurement 55 (2014) 571–580

Contents lists available at ScienceDirect

Measurement

journal homepage: www.elsevier.com/locate/measurement

Measurements of diffusion coefficients in solids by means of LIBS combined with direct sectioning

C. Ararat-Ibarguen [a], R.A. Pérez [a,b,c,*], M. Iribarren [a,c]

[a] Departamento de Materiales Comisión Nacional de Energía Atómica (CNEA), Avenida General Paz 1499, B1650KNA San Martín, Pcia. de Buenos Aires, Argentina
[b] CONICET (Consejo Nacional de Investigaciones Científicas y Técnicas, Argentina
[c] Instituto Sabato, UNSAM/CNEA, Argentina

ARTICLE INFO

Article history:
Received 18 March 2014
Received in revised form 14 May 2014
Accepted 9 June 2014
Available online 21 June 2014

Keywords:
Diffusion coefficient
LIBS
Direct sectioning

ABSTRACT

This work explore the application of Laser Induced Breakdown Spectroscopy (LIBS) to the measurement of diffusion coefficients D in solids. Different experimental set ups were tested looking for minimize the error and extend the range of D values achievable. It was found that the combination of direct sectioning with precision grinder plus LIBS is the best arrangement in order to fulfill these goals. Excellent agreement with previous results in the literature, measured with standard techniques, was obtained.

1. Introduction

Despite the early works studying the chemical diffusion process (e.g. by Kirkendall et al. [1]) determination of diffusion coefficients (D) at infinite dilution in solids, in particular metals, was not developed until the 1950s decade when radiotracers became available in science labs.

Several experimental methods were developed which can be grouped in two categories: direct mostly, requiring the use of radiotracers, and indirect, which usually does not require radiotracers.

The indirect methods take advantage of the fact that many physical phenomena in solids depend on the occurrence of thermally activated motion of atoms. Then from a suitable measurement of such phenomena, diffusion coefficients can be determined; however the results could be strongly modelling dependent and, moreover, these methods are often sensitive to only one or to a few atomic jumps, consequently it is not unlikely to over or under estimate the values of effective diffusion coefficients.

The direct methods are based on fitting the diffusant concentration C in Fick's law:

$$\frac{\partial C}{\partial t} = \frac{\partial}{\partial x}\left(D\frac{\partial C}{\partial x}\right) \tag{1}$$

where x is the distance travelled by the diffusant during a given time t at a given temperature.

Here, diffusion occurs over distances which are large compared to the interatomic distance. One measures either a diffusion flux, an integrated diffusion flux, a concentration profile or an integrated concentration profile. In this context, permeation experiments through a membrane involving steady-state solutions to Fick's law, surface activity decrease, autoradiography and several other methods were applied to the measurement of diffusion coefficients. However the more frequent and more accurate methods used to obtain the bulk of the diffusion data until 1990 compiled e.g. in Ref. [2], were the direct profile measurement and Gruzin-Seibel's technique (c.f. Ref. [3] for a

* Corresponding author. Address: Gerencia de Materiales Comisión Nacional de Energía Atómica (CNEA), Avenida General Paz 1499, B1650KNA San Martín, Pcia. de Buenos Aires, Argentina. Tel.: +54 11 6772 7749; fax: +54 11 6772 7262.
E-mail address: rodperez@cnea.gov.ar (R.A. Pérez).

http://dx.doi.org/10.1016/j.measurement.2014.06.009
0263-2241/

complete description). Both introduce the diffusant through a thin layer of radiotracer deposited on a plane surface of the sample. Vacuum evaporation, electrochemical or chemical deposition and ion implantation are the most common deposition techniques. Starting form this condition, after annealing at a given temperature, during a known time t, the diffusant redistribution is given by a simple solution of Eq. (1): a Gaussian function if the solubility in the matrix is large enough:

$$C(x,t) = \frac{\alpha}{(4\pi Dt)^{1/2}} \exp\left(-\frac{x^2}{4Dt}\right) \quad (2)$$

or a complementary error function if the solubility is low.

$$C(x,t) = C_S[1 - \mathrm{erf}(x/(4Dt)^{1/2})] \quad (3)$$

where α is the initial amount of diffusant per unit area; C_S stands for the solubility limit and erf means error function.

Direct sectioning with radiotracer is preferred, if possible. In this case, after the diffusion anneals the profile $C(x)$ is determined by sectioning the diffusion zone and measuring the activity (related to the tracer concentration) in each section. If, for instance, the solubility is large enough and then Eq. (2) applies, the tracer diffusion coefficient D may be determined from $\ln(C)$ vs x^2 plot leading to a straight line with slope $-1/(4Dt)$. The excellent linearity usually obtained allows a determination of D within a few percent accuracy.

Serial sectioning can be performed with several tools: precision lathe (10 μm; 5×10^{-16} m^2 s^{-1}), a microtome (1 μm; 10^{-17} m^2 s^{-1}) or a precision grinder (0.5 μm; 5×10^{-18} m^2 s^{-1}) the numbers within parentheses indicating the minimum section thicknesses and the minimum diffusion coefficients attainable with each tool. Section thickness, thus the penetration distance, is usually measured by weighing.

The direct sectioning with radiotracers has two main limitations. The first one is the minimum D attainable. Diffusion coefficients below 5×10^{-18} m^2 s^{-1} require forbiddingly large annealing times to obtain large enough radiotracer penetration in order to apply the method.

As D depends on temperature T thorough Arrhenius law:

$$D(T) = D_0 e^{-\frac{Q}{kT}} \quad (4)$$

(where Q is the activation energy, k the Boltzmann constant and D_0 a pre-exponential factor related with the vibrational entropy of the system) D values below 5×10^{-18} m^2 s^{-1} already come out roughly at temperatures below $T_m/2$ (being T_m the matrix melting temperature); range where most of the technological processes happen. Measurements at higher temperatures can be used to obtain Q and D_0 via extrapolation of Eq. (4) to lower ones, but due to the exponential behaviour a significant uncertainty may arise, and even worse, some important metals (such as Fe, Ti and Zr) present allotropic phase transitions below $T_m/2$ that inhibit the extrapolation.

This problem was solved when sub-micrometric sectioning techniques became available: sputtering by bombarding with ions (5 nm; 10^{-22} m^2 s^{-1}) and chemical or electrochemical attack (2 nm; 5×10^{-24} m^2 s^{-1}) though at the cost of reduced precision.

The second restriction for direct sectioning with radiotracers lies in the need to have an appropriate radiotracer in order to perform the experiment, that means one with a mean lifetime large enough (at least several months) emitting a suitable kind of radiation, essentially electromagnetic (γ, X-ray). For radiotracers that emit particles (β, α, conversion electrons) Gruzin-Seibel's method is used, where essentially, the activity of the remaining material (instead the one in the removed layer) is measured [3].

In the context of this limitations, the association of ionic sputtering for sectioning with secondary ion mass spectrometry (SIMS), secondary neutral mass spectrometry (SNMS) or Auger electron spectroscopy (AES) in commercial analyzers, allows the measurement of diffusion coefficients without the need of radiotracers. Also non-destructive techniques that use ions as analysis tool, such as Rutherford Backscattering Spectrometry (RBS), Heavy Ion RBS (HIRBS) and Nuclear Reaction Analysis (NRA), all involving the use of small and medium particle accelerators are capable to measure diffusion coefficients with non-radioactive diffusants.

All these techniques require, however, expensive and complex facilities; compared to them, the Laser Induced Breakdown Spectroscopy (LIBS) basic equipment, like the used in the present work, is a relative cheap device with a simple handling and installation.

LIBS is an analytical technique based on the application of one or more high power laser pulses on a reduced region of the sample surface, promoting ablation and excitation of the specimen with the formation of a transient plasma. In the subsequent cooling time, the plasma produces both continuous and discrete emissions which are collected by a spectrometer providing the corresponding emission spectra of the sample [4].

Even though LIBS has already been used to measure diffusion coefficients e.g. [5,6] in what we call the *single crater mode* (see Section 4.1 further on), the goal of the present work, after analyzing several alternatives, is to improve the experimental set ups by combining direct sectioning via a precision grinder with LIBS as analysis tool in order to measure non-radioactive diffusant concentrations layer by layer.

2. Sample preparation and diffusion couples's conformation

As a test case, we determine diffusion coefficients of Cr and Fe (basic constituent of stainless steels) in the Zr–2.5 wt%Nb (Zr–2.5Nb) alloy, the material used in pressure tubes of CANDU nuclear reactor. Besides their interest in the nuclear industry, we choose those diffusants because there are data in the literature regarding diffusion in pure β-Zr showing at least 3 orders of magnitude difference between Cr [7,8] (slower) and Fe [9] (faster); this difference will help us to test several ways to get diffusion profiles with LIBS.

The base material were plates ($0.5 \times 1.0 \times 0.3$) cm of Zr–2.5Nb alloy (ATI Wah Chang, ASTM B 353-02 – R60901) whit the following composition: Nb 2.4–2.8%;

O: 0.09–0.13%: Al: 75 ppm; Fe; 1500 ppm; Cr; 200 ppm, Ti 50 ppm and U 3.5 ppm as given by the manufacturer.

The samples show very fine grains of α-Zr phase surrounded by a thin layer of β-Nb, oriented in the longitudinal direction of the pressure tube. In order to homogenize and increase the grain size; they were subject to a heat treatment of 3 h at 1243 K, at this temperature both Zr and Nb are in solid solution in the bcc β-phase, finally they were temperate.

The samples were mechanically polished in order to get flat and parallels surfaces and then mirror polished in a mechanical–chemical arrangement using a polishing cloth soaked with potassium dichromate and 0.05% HF in aqueous solution.

Cr and Fe were introduced by dropping $Cr(NO_3)_3$ and $FeCl_3$ in aqueous solutions onto the polished Zr–2.5Nb samples and then drying with an IR lamp.

Diffusion anneals were performed under dynamic vacuum, $2 \cdot 10^{-6}$ torr, temperatures were controlled within ±1 K with Pt–PtRd S type thermocouples.

The weighing of the removed layers (see Section 4.3) was performed using a Metzler scale capable of 5×10^{-5} g precision.

3. Setting up LIBS parameters

Once the diffusion couples were built, an Ocean Optics LIBS 2500 plus™ equipment was used to determine the constituents proportional concentration. The equipment has a Nd:YAG laser which delivers 50 mJ Q-switched pulses at 1064 nm, with variable repetition rates from 1 to 20 Hz. At 1064 nm the laser pulse stability is ±3%.

The beam parameters, at 98% of maximum energy are: near field beam diameter 2.46 mm, pulse width-FWHM 5.41 ns, divergence at 86.5% 0.56 mrad. Data given by manufacturer.

The last stage in the laser beam focus is made using a lent ACH-NIR 25×60 NIRII p of 60 mm focal distance, mounted in the chamber as shown in Fig. 1.

The emitted light is collected with an optical fiber (see Fig. 1 for details) connected to three channel CCD detectors (HR2000+) covering the wave length range between 200 and 525 nm. The spectral resolution is ~0.1 nm, less than this in the UV-blue and a bit higher in the red-IR.

Our first task was to choose the right ablation and detection parameters of our equipment, for the given samples, in order to get a proper spectrum. With the reported set up of the equipment, the laser-induced plasma starts as very hot 15,000 K plasma [4], emitting a large bremsstrahlung continuum. Depending on the sample matrix, most emission analysis must be performed several microseconds after initial plasma generation, in order to avoid the continuum masking of the line structure. The optimal retarding time $\mathbf{t_d}$ (time before activation of the spectrometer acquisition) was chosen as 155 μs, the acquisition time $\mathbf{t_g}$ as 10 μs, being the laser pulse of 10 ns.

A typical spectrum for the Zr–2.5Nb matrix, without diffusant, is shown in Fig. 2a. During the acquisition time, the higher order transitions decay away, leaving mostly I and II atomic emissions. These are the ones that were identified using the spectral library consisting of 2500 atomic emission lines from the NIST (National Institute of Standards and Technology) tables for elemental identification. In Fig. 2a the corresponding spectral lines for both Zr and Nb are shown, several other spectral lines can be observed corresponding to other constituent elements and impurities present in the alloy; such complex spectrum is typical for metals, even for the purest ones.

At this point it is essential to choose a proper line or set of lines of Cr to be used in order to analyze and determine the total amount of diffusant present in the ablated portion of the sample, the straightforward election of the more intense line, as given by NIST, is not the better choice, since it could by convoluted with one or several matrix lines. Then, by proper we mean a spectral line with a large enough intensity with respect to the background and separate from the matrix lines in order to avoid convolution with them, since the amount of diffusant is low compared with the matrix constituents and could be entirely masked even by their lest intensive lines. In the present case we choose the Cr I line at 425.43 nm; a zooming spectrum around this line is shown in Fig. 2b.

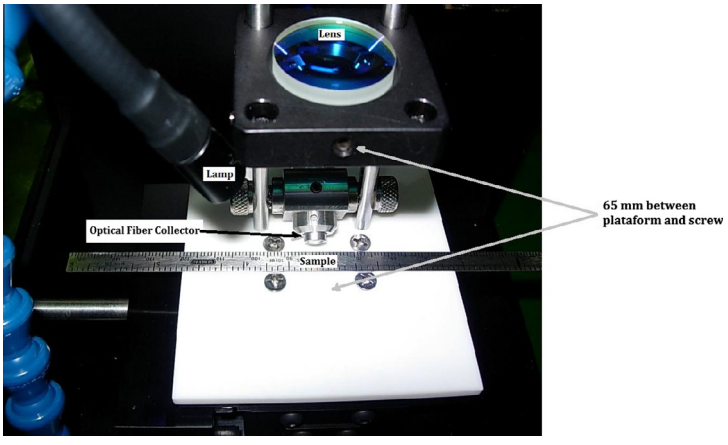

Fig. 1. Optical focus and collection in LIBS 2500 plus™.

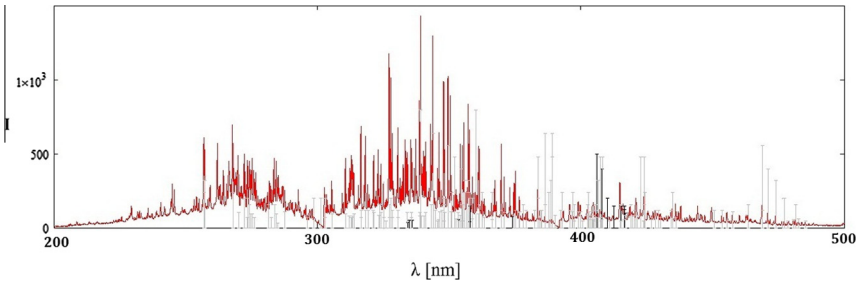

Fig. 2a. LIBS spectrum for Zr2.5Nb. Grey lines correspond to Zr spectral lines, black lines to the Nb ones.

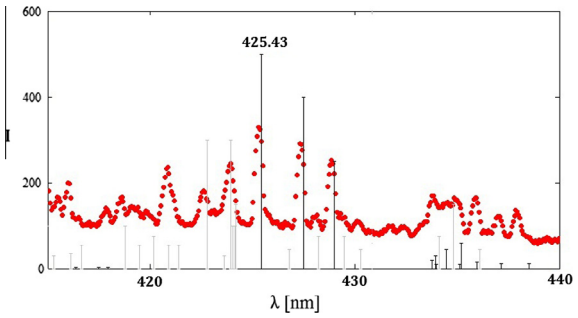

Fig. 2b. LIBS spectrum for Zr2.5Nb with Cr thin layer deposited onto the surface, zoomed around the 425.43 nm Cr line. Grey lines correspond to Zr spectral lines, black lines to the Cr ones.

A similar analysis for Fe leads us to choose its 374.56 nm spectral line.

4. Measurements of the diffusion profiles

After the diffusion annealing the diffusant redistributes into the sample following Eq. (2) in both cases, Cr and Fe, since their solubilities are large enough. The usual way to get D from this equation is to measure the diffusion profile, that means a list of Cr/Fe concentration C for each depth x measured from the deposition surface. We explore three different ways to get such profile:

4.1. Single crater measurement

We began the measurements applying the method reported in the literature [5,6] used in order to get diffusion profiles. The laser beam impinges perpendicular to the deposited surface, parallel to the diffusion direction. Several consecutive shots at the same spot develop a single crater. After each shot the corresponding spectrum is collected, the x coordinate is determined by measuring the sputter crater total depth and the ratio between the total and the corresponding number of shots.

In order to explore the laser shot effects regarding homogeneity and repeatability onto the sample, we have analyzed different craters sputtered with different numbers of shots. Also we performed a calibration of the number of shoots against depth x.

Fig. 3 is a micrography with the craters formed in Zr2.5Nb after different number of shots, from 2 to 60 given by a microscope OLYMPUS Confocal model LEX OLS 3000 which allows us to obtain three-dimensional images and to perform a crater depth determination by interferometry with a resolution of 0.12 μm. The zoomed detail in Fig. 2 shows crater morphology and width after 60 shots given by a SEM microscope. Fig. 4 shows a quite nice linear correlation between number of shots and depth.

Laser shots are not homogenous as shown in Fig. 3. On one hand, the energy deposited by the laser beam has a certain scatter, being the amount of ablated sample not uniform; consequently, the area under the Cr/Fe peaks must be normalized to take this effect into account.

On the other hand, the crater's diameter changes from several tens of μm to around 600 μm when the number of shots increases (after 60 shots diameters remain almost constant); consequently the crater has a kind of conical tip shape; also some re-deposition of the ablated material take place.

All these effects, that happen when successive laser shots are delivered onto the same spatial point on the sample surface, are very well known and were also observed in the previous works [5,6] given origin to a convoluted signal since a fraction of the material coming from previous shot is unavoidable mixed in the signal of the next one.

These is the reason why we explore in Sections 4.2 and 4.3 other experimental arrangements searching for improve the measurements, narrowing the experimental error.

In order to reduce the dispersion observed in the data, probably coming from the mentioned mixing problem and given the large number of spectra collected, we average each sets of 10 shots with a better result.

There are several ways to normalize the Cr/Fe signal with respect of the total amount of ablated material after each shot; the simplest one is to make a ratio between the area under the Cr/Fe peaks selected in Section 3 and the total spectrum area; However, in order to minimize the noise effect in the profiles, after several tries we found it better to perform a ratio between the area under the Cr/Fe peaks and the sum of the areas under a set of several Zr peaks: the ones located between 422.1 and 424.6 nm. This is valid in studies of diffusion at infinite dilution, as is the present case, where the amount of diffusant is negligible, so the amount of Zr (the major component in the alloy) remains virtually constant at all depths:

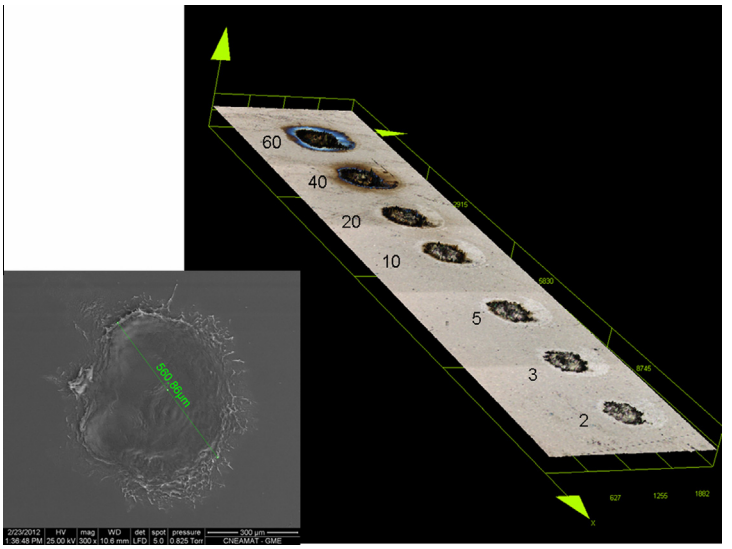

Fig. 3. Optical microscope image for the sample surface after different number of lasers shots. The zoomed SEM image corresponds to the 60 shots hole.

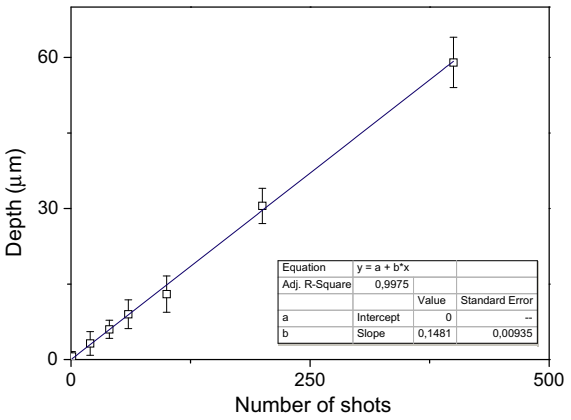

Fig. 4. Calibration number of shots against depth for Zr2.5Nb samples.

$$C(x) = I[Cr(\lambda = 425.43)]/I[Zr(\lambda = 422.8)] + I[Zr(\lambda = 423.9)] + I[Zr(\lambda = 424.1)] \quad (5)$$

In other cases, when the amount of diffusant is significant, its contribution has to be taken into account:

$$C(x) = I[Cr(\lambda = 425.43)]/I[Zr(\lambda = 422.8)] + I[Zr(\lambda = 423.9)] + I[Zr(\lambda = 424.1)] + I[Cr(\lambda = 425.43)] \quad (6)$$

Similar equations can be used for I[Fe(λ = 374.56).

In the present case, there are not substantial differences between the use of Eqs. (5) and (6). At this point is important to remark that $C(x)$ is measured in arbitrary units proportional to the lines intensities. The denominators in those equations are only for standardize the signal with respect to the energy deposited onto the sample by shot, not to make an absolute calibration.

The Fig. 5a shows the normalized Cr peaks against the number of shots after a diffusion anneal of 1 h at 1173 K, they decrease with the number of shots until reaching the background, as expected. Then the graphic in Fig. 6a: namely, peak intensity against number of shots, has a Gaussian shape.

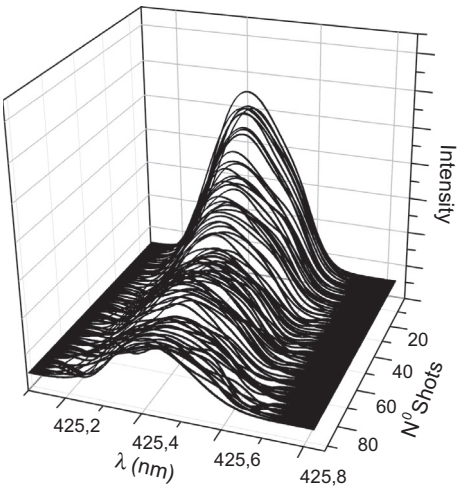

Fig. 5a. Spectra shot by shot zoomed on the Cr peak.

In order to verify that this is not an artifact of the measurement conditions, in Fig. 5b we show normalized Nb peaks (λ = 415.02 nm) against number of shots; it is clear that the signal reminds almost constant, as expected, since Nb is a minority component in the matrix alloy whose composition does not change.

The linear behaviour found in Fig. 4 let us to straightforwardly convert the number of shots into depth x by applying the formula: shoot number times (crater depth/total number of shots).

A good linear fit of: ln I vs x^2, (full line) is observed in Fig. 6b, thus from Eq. (2), where the annealing time is t = 3600 s, a diffusion coefficient for Cr in Zr2.5Nb at

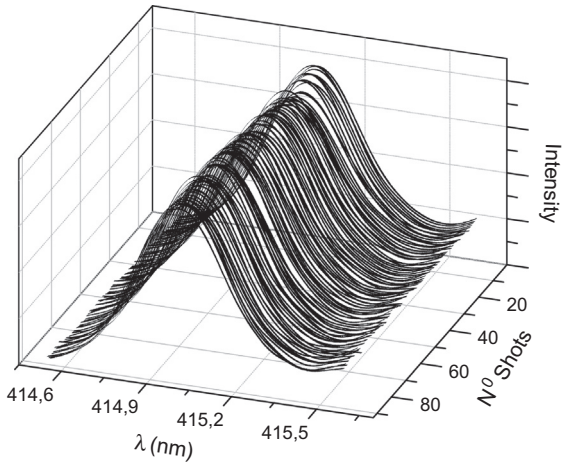

Fig. 5b. Spectra shot by shot zoomed on the Nb peak.

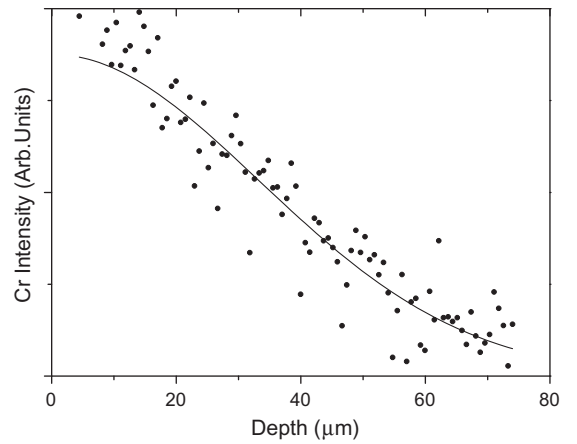

Fig. 6a. Cr Intensity against depth after 1 h anneal at 1173 K. Single crater arrangement.

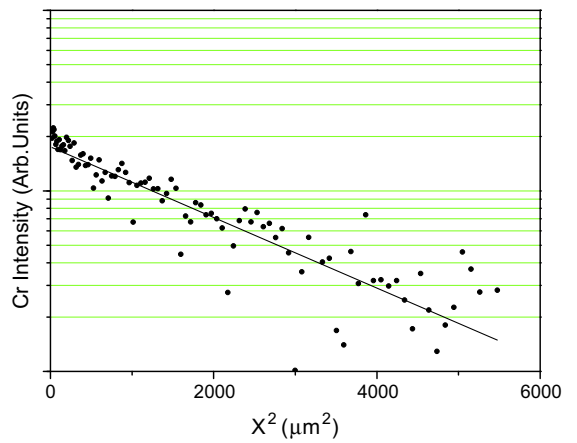

Fig. 6b. Cr diffusion profile in logarithmic scale after 1 h anneal at 1173 K. Single crater arrangement.

1173 K of $^{Zr2.5Nb}\boldsymbol{D}^{Cr}_{1123K} = 3.5 \times 10^{-14}$ m^2/s is obtained from the slope.

The same procedure is applied to a sample with Fe diffusant layer; after a diffusion annealing of also 1 h at 1173 K. Fe peaks intensity against number of shots is now shown in Fig. 7a. Fig. 7b is the corresponding ln I vs x^2 plot. As expected from the diffusion data in pure β-Zr [9], Fe diffusion results orders of magnitude faster than Cr diffusion [7,8]. Let is note that, by analyzing Eq. (2), the maximum amount of Fe per unit area, after annealing, is the one at the surface ($x = 0$) given by $\alpha/(4\pi Dt)1/2$. Therefore the highest the $(Dt)1/2$, the lowest the maximum amount of Fe detectable, thus the ratio signal/noise for the faster diffuser is poor. Consequently the mixing problem referred above becomes more significant, leading to the scattered spectrum shown in Fig. 6a, barely above the noise.

Nevertheless, from the slope of Fig. 7b, it is possible to obtain $^{Zr2.5Nb}\boldsymbol{D}_{1123K}\mathrm{Fe} = 2 \times 10^{-11}$ m^2/s, but with an error well above 50% (see discussion in Section 5).

4.2. Lateral side measurement

In this case the laser beam impinges on a lateral side of the samples, perpendicular to the diffusion direction. The sample is mounted on a mobile platform attached to a micrometer screw, in our case it was moved in steps of 20 μm from the deposition and along the diffusion direction. Twelve shots at each spot were made (discarding the first two in order to avoid eventual dirt deposited onto the lateral surface); the mean spectra were then saved.

Given the optical arrangement used in the LIBS 2500 plus TM equipment, the one given by the manufacturer and reported above, the crater diameter is of around 80 μm; the actual shape of the spot is shown in the photography in Fig. 3, the one corresponding to 10 shots. A kind of Olympic rings shape was formed; consequently the signal analyzed becomes mixed and convoluted.

As the x coordinate is simply determined by the number of steps of the micrometric screw, Fig. 8a is directly the Fe peak intensity against x. Fig. 8b is the corresponding ln I vs

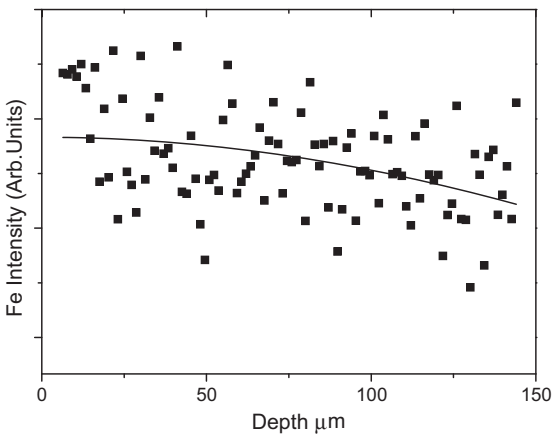

Fig. 7a. Fe intensity against depth after 1 h anneal at 1173 K. Single crater arrangement.

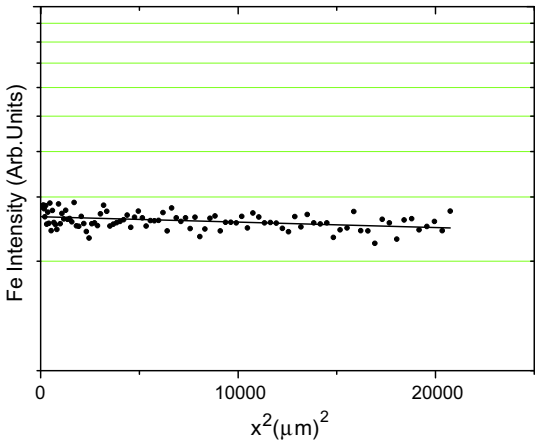

Fig. 7b. Fe diffusion profile in logarithmic scale after 1 h anneal at 1173 K. Single crater arrangement.

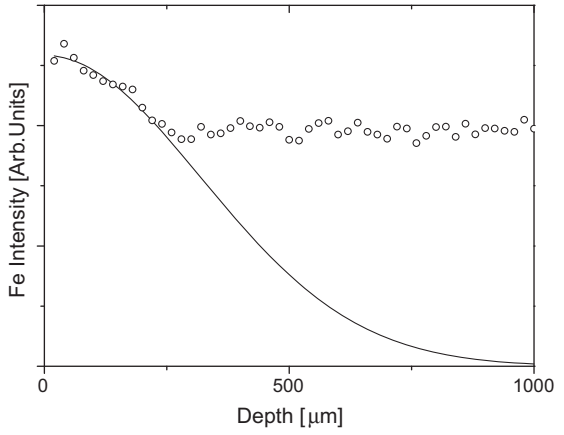

Fig. 8a. Fe intensity against depth after 1 h anneal at 1173 K. Lateral side arrangement.

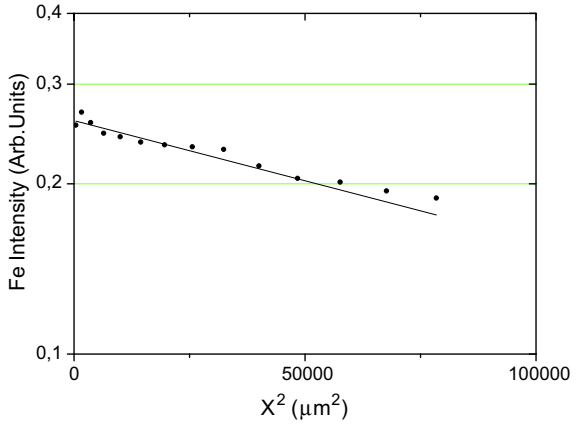

Fig. 8b. Fe diffusion profile in logarithmic scale after 1 h anneal at 1173 K. Lateral side arrangement.

x^2, both graphs correspond to the same sample analyzed in Section 4.1.

From the slope of the last figure a D value of ${}^{Zr2.5Nb}\boldsymbol{D}_{1123K}Fe = 2 \times 10^{-11}$ m^2/s is obtained, but let is note that the profile in the logarithmic scale decay less than a decade, which is reflected in the data fit show as a full line in Fig. 8a. In order to do such fit, we impose the Gaussian solution Eq. (2) to the first 14 points discarding the remained ones, using as the square width $(4Dt)1/2$ the value obtained from Fig. 8b slope. In this way it is clear that the measured data only correspond to the upper part of the Gaussian, the remained part was merged by the mixing onto the noise.

In the case of the Cr sample, the Gaussian width $(4Dt)1/2$ is around 20 μm, thus all the profile information lies just in the first shot, becoming unobservable whit this experimental setup. In order to get a good diffusion profile at least 10 (preferably more) points are required, meaning an annealing time of several hundred hours must be done in order to observe such kind of profiles for Cr diffusion at this temperature.

Those limitations can be partially avoided by changing the optical focus device provided by the manufacturer for a more precise one, capable of to narrower diameter spots. We neither explored this option nor extended the annealing time given the findings in the next section.

4.3. Direct sectioning with precision grinder

In this arrangement the sample is glued onto a support capable of fitting on a rotary head; the head is used to align the sample surface parallel to a flat mobile platform and then remains fixed for the rest of the experiment. An abrasive paper of chosen granulometry is glued to the platform, so the reciprocating motion of that platform allows thin layers of the sample to be removed (from 0.5 to several tens of μm, according to the abrasive paper and the number of cycles of the motion), at least until remove any trace of the previous laser holes.

The sample together with the support can be removed from the rotary head, transported to a scale, weighed in order to know the amount of removed material (by difference with a previous measurement), shoot with the laser

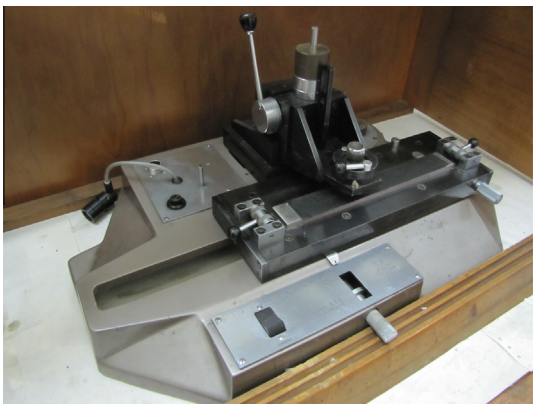

Fig. 9. Precision grinder.

beam in order to know the amount of diffusant present in the new surface, and finally reset at the head in the exact same position. A photo of the precision grinder is shown in Fig. 9.

We begin measuring the surface diffusant concentration by shooting 10 times at 50 different spots in the surface; the first 2 shots are discarded (they just clean the surface) and the mean of the 8 remaining spectra is saved. The area under the diffusant peak, weighted by the area under the Zr peaks are calculated (as related in 4.1) for the 50 spots; finally the mean value of those areas is taken as the diffusant concentration, in arbitrary units, at the surface $C(x = 0)$.

A layer is removed in the grinder and its thickness is determined by weighing and knowledge of the area A and density ρ of the sample, then for the nth layer:

$$x_n = \sum_{i=1}^{n-1}(x_i) + \frac{(p_n - p_{n-1})}{\rho \boldsymbol{A}} \tag{7}$$

being p_n the weigh of the sample plus the support after n cycles.

Finally the whole process is repeated until the area under the diffusant peaks merge onto the background.

In this way a considerable improvement in the signal/noise ratio is obtained, as can be seen in Fig. 10a: Diffusant concentration against x for the same sample measured in 4.1 and 4.2, the one with the Fe deposit annealed in Zr2.5Nb 1 h at 1173 K.

From the slope of Fig. 10b now we get ${}^{Zr2.5Nb}\boldsymbol{D}_{1123K}$ Fe $= (1.10 \pm 0.05) \times 10^{-11}$ m^2/s. The diffusion profiles vary one and a half decades in the logarithmic scale and the Gaussian fit in Fig. 10a is improved when compared with the one in Fig. 8a.

5. Data analysis and discussion

When comparing the three experimental arrangements, the gain in combining the precision grinder with LIBS becomes clear if we first analyze the magnitude of the errors made in D determination for each different method

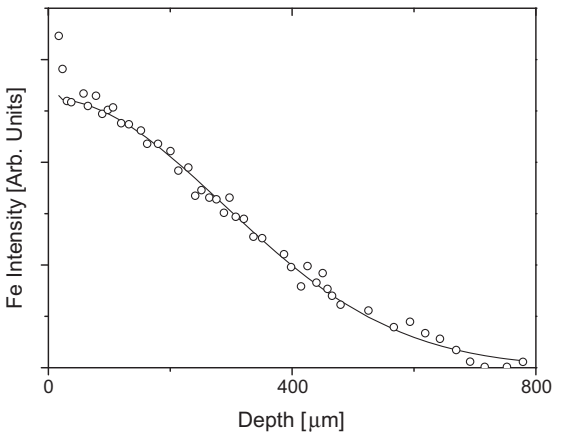

Fig. 10a. Fe intensity against depth after 1 h anneal at 1173 K. Direct sectioning with precision grinder arrangement.

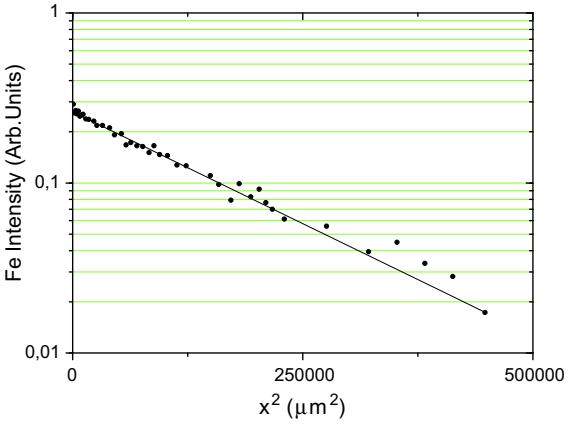

Fig. 10b. Fe diffusion profile in logarithmic scale after 1 h anneal at 1173 K. Direct sectioning with precision grinder arrangement.

and then we determine the range of D measurable in each one.

In the single crater analysis we have two cases: for Cr diffusion a good signal/background ratio was achieved, then the $\ln(C)$ vs x^2 shown in Fig. 6b drops one decade with statistical error on the slope of 8%. For diffusing Fe there is a worst signal/background ratio, part of the Gaussian merges into the background, consequently the drop in the fit in Fig. 7b is less than one tenth of a decade and the statistical error calculated for the slope is 25%. Let is see how all those elements add to the total error in D.

It is easy to see that the percent error $(\Delta D/D) \times 100\% \equiv \Delta D\%$ equals $(\Delta s/s) \times 100\% \equiv \Delta s\%$, where s is the slope in the $\ln(C)$ vs x^2 fitting line and Δs its corresponding error.

On the other hand $\Delta s\%$ is made out of the addition of the statistical error plus the one coming from the propagation of the errors incurred in x and C experimental determination. A rough estimation of the latter can be made by approximately taking s as:

$$s \approx \frac{\ln C(x) - \ln C_0}{x^2 - x_0^2} = \frac{\ln(C/C_0)}{x^2} \tag{8}$$

where C_0 is the diffusant concentration at $x_0 = 0$. Then:

$$\Delta s\%_{exp} \approx \frac{\Delta C\%}{|\ln(C/C_0)|} + 2\Delta x\% \tag{9}$$

where $\Delta C\%$ $(\Delta C/C) \times 100\%$ is the percent error in the determination of the diffusant concentration and $\Delta x\%$ the corresponding one for depth. When the drop in C with respect to C_0 is one order of magnitude $\ln(0.1) = 2.3$ and the influence of $\Delta C\%$ diminishes by approximately half, but when the drop is only a tenth of C_0, $\ln(0.9) = 0.1$, thus $\Delta C\%$ increases one order of magnitude and becomes dominant.

Determination of the C experimental error is not straightforward since not quantitative, but relative, measurements were made in the present case (for instance, it is impossible to contrast against a standard). If we consider a rather optimistic $\Delta C\%$ of 10%, in the measurements of Fe diffusion with the single crater method, since C/C_0 is 0.9, its

contribution to $\Delta s\%$ through Eq. (9) is 100%. A 25% statistic error plus $\Delta x\%$ have to be added, which means that the value obtained with this method for $^{Zr2.5Nb}\boldsymbol{D}_{1123K}$Fe is only an order of magnitude indication of the diffusion processes.

For Cr diffusion, also measured with the single crater method, a significant improvement is observed. In fact, since C/C_0 is 0.1 the contribution of $\Delta C\%$ to the total $\Delta s\%$ error is reduced to less than a half (exactly 2.3^{-1}). In order to estimate Δx for this method we have to take into account that even when the nominal resolution of the OLYMPUS microscope is 1.2 μm, it is only valid when two flat surfaces at different depth are compared; in our case the conic tip of the crater modifies such resolution in at least half order of magnitude. Consequently, $\Delta x\%$ rises from a nominal 1% to at least 5%.when a crater of few hundred of μm depth is measured.

The consideration of both contributions through Eq. (9) obtains $\Delta s\%_{exp}$ between 10% and 15%. With the addition of the statistical error coming from the least square fit of Fig. 6b (8%), the total $\Delta s\%$ lies between 20% and 25%. This is the error for the method described in Section 4.1, obtained in the best experimental conditions and assigning a rather optimistic error of 10% to C determination.

Let is now compare with the data in the literature for pure β-Zr. In [7] 51Cr diffusion in β-Zr was measured in the temperature range of 1187–1513 K using serial sectioning with precision grinder. Extrapolation to 1173 K from them gives 3.2×10^{-13} m^2/s. In [8] 51Cr diffusion in β-Zr was measured using lathe sectioning but in a higher temperature range 1557–1950 K. Extrapolation from [8] to 1173 K is 5.5×10^{-14} m^2/s. Our measurement obtained with the single crater arrangement $^{Zr2.5Nb}\boldsymbol{D}_{1123K}$Cr = $(3.5 \pm 0.9) \times 10^{-14}$ m^2/s is closer to the latter tough inside the range in between both.

Let is apply the same analysis to the lateral side measurement described in 4.2. To assign $\Delta C\%$ a value lower than 10% is more realistic than in the previous case: the data plotted in Fig. 8a has a considerable lower dispersion than the one plotted in Fig. 7a; even when we still have a mixing problem with this method, the reason of such improvement comes from the fact than an average of ten measurements of the same quantity at each spot was made. Nonetheless the low drop in Fig. 8b still makes the contribution of $\Delta C\%$ dominant in this measurement.

On the other hand, the main contribution to $\Delta x\%$ comes from the exact determination of the spot corresponding to the surface; it takes one shot of uncertainty to do that. In the present case, after around 250 μm the signal becomes merged into the background, so the error is 8%. In optimal conditions the depth analysis may be extended and $\Delta x\% = 5\%$ may be achieved.

Consequently, in the optimal conditions, with at least one decade drop in the ln (C) vs x^2 plot and a statistical error between 5% and 10%, the total error for the lateral side measurement (Section 4.2) is $\Delta D\% \approx 20\%$.

For the last case (Section 4.3), when direct sectioning with precision grinder is used, the improvement in the error determination is significant. On one hand, it is easy to prove (from Eq. (7)) that $\Delta x/x = 2\Delta p/p$, where p is the weight of the sample's portion removed, in the present case p was 0.2 g at the maximum depth analyzed (≈700 μm). Given the precision of the Metzler scale used for weighing (5×10^{-5} g), the contribution of $\Delta x\%$ in Eq. (9) is negligible. For further measurements performed at shallower depths, the same condition can be achieved by increasing the area of the departure sample.

On the other hand, C is determined by an average of 400 measurements, at 50 equivalent spots, of the same quantity for each depth x and all the mixing problems presented in the previous experimental arrangements are completely avoided. Again, the assignment of a value to $\Delta C\%$ is an estimation, but given the increase in the statistics and the low dispersion in the data observed in Fig. 10a, it may not be larger than a few percent, say no more than 3% in order to simplify the calculations; since the drop in Fig. 10b is almost a decade and a half and $\ln(0.05) = 3$, the contribution to the total error could be, at worst, 1%.

Adding the statistical error coming from the least square fit in Fig. 10b of 3%, the total percent error $\Delta D\%$ in the determination of diffusion coefficients using LIBS combined with precision grinder is now less than 5% (actually between 3% and 4% in the present measurement) which is the usual error assigned to standard techniques used to measure diffusion coefficients such as those of the introduction section.

Finally, let is compare the results here obtained with data in the literature. In [9] 59Fe diffusion in β-Zr and β-Zr Nb alloys was measured in the temperature range between 1176 and 1886 K using lathe sectioning. Extrapolation of these values to 1173 K gives Zr$D = 1.15 \times 10^{-11}$ m^2/s in excellent agreement with the result here obtained by using LIBS plus grinder $(1.10 \pm 0.05) \times 10^{-11}$ m^2/s. On the other hand, the result obtained from the other two methods is a common 2×10^{-11} m^2/s, but the larger than 100% error bar includes all three in the same range. The factor two may probably be related to the mixing problem mentioned before, namely, part of the material with the richest content of diffusant content is assessed as belonging to deeper region of the sample; nevertheless either with the single crater or the lateral side measurement a reasonably good guess of the actual D value is obtained.

Besides the error reduction, the use of LIBS plus grinder allows us to increase the range of measurable D values with respect to the other two methods.

In fact, in order to get a good profile with at least one decade drop in the ln(C) vs x^2 plot, the minimum total depth to analyze in each experimental arrangement must be, at least, twice the Gaussian width: $2\sqrt{4Dt} = x_{min}$. As already said, in order to get a good fit, at least 10 points are needed, which means in the lateral side method $x_{min} = 200$ μm, in the single crater x_{min} around 60–100 μm, and for LIBS plus grinder $x_{min} = 5$ μm.

On the other hand, a maximum annealing t_{max} reasonable enough in order to obtain a result of around 10^7 s (a bit longer than 3 months) lowers the minimum D_{min} achievable in each arrangement (note that, given the square root relationship with time, in order to increase x_{min} by a factor of 10, the time must be increased in 100, that means 300 months anneal, by all means impractical).

Considering altogether, D_{min} for each arrangement is given by:

$$D_{min} = \frac{x_{min}^2}{4t_{max}} \quad (10)$$

amounting to 5×10^{-16} m^2/s for the lateral side arrangement, 10^{-16} m^2/s for the single crater one, and 5×10^{-18} m^2/s for LIBS plus grinder.

As was pointed out in the text, it is possible to improve the experimental arrangements presented in Sections 4.1 and 4.2 by using more expensive lasers and detection systems, and better optical configurations in order to focus the beam in narrower spots; however, the main objective of this work was to use the relatively cheap basic equipment, as given by the manufacturer, with a simple handling and installation, in order to measure diffusion coefficients with the same precision and accuracy than the standard methods applied in classical diffusion coefficient measurements.

6. Conclusions

Standard LIBS equipment was used in order to measure diffusion coefficients D in metals. Three experimental arrangements were analyzed.

The combination of the direct sectioning method using a precision grinder with LIBS measurements, presented here for the first time, becomes the best choice. It minimizes the error rate to less than 5% and extends the minimum measurable D values to 5×10^{-18} m^2/s.

Those conditions can be achieved by using standard equipment as sold by the manufacturer with no need of complex or expensive modifications.

Comparison among the values obtained here with data in the literature using other measurement methods obtains excellent agreement.

Acknowledgments

This work was partially supported by the Consejo Nacional de Investigaciones Científicas y Técnicas CONICET PIP 0804/10 and by the Agencia Nacional de Promoción Científica y Tecnológica PICT.

References

[1] T.D. Kirkendall, L. Thomassen, C. Upthegrove, Trans. AIME (1939); A.D. Smigelskas, E.O. Kirkendall, Trans. AIME (1947).
[2] H. Meherer, Diffusion in Solids, Springer-Verlag, Berlin Heidelberg, 2007. pp. 39–41.
[3] Y. Adda, J. Philibert, La diffusion dans les solides (Institut National des Sciences et Techniques Nucléaires – Saclay-France 1966) vol. 1, Chap. 3 pp. 253–265.
[4] A. Miziolek, V. Palleschi, I. Schechter, Laser-Induced Breakdown Spectrometry (LIBS) Fundamentals and Applications, Cambridge University Press, Cambridge, UK, 2006.
[5] C.-G. Lee, K.-T. Youn, Y.-I. Lee, D.-S. Yoo, T. Shimozaki, Defect Diffusion Forum 194–199 (2001) 79–84.
[6] C.-G. Lee, J.-H. Lee, B.-S. Lee, Y.-I. Shimozaki, T. Okino, Defect Diffus. Forum 237–240 (2005) 266–270.
[7] L.I. Nicolai, R. Tendler, J. Nucl. Mater. 87 (1979) 401.
[8] R.H. Zee, J. Phys. Condens. Matter 1 (1989) 5631.
[9] C.H.R. Herzig, J. Nehaus, K. Vieregge, L. Manke, Fast impurity diffusion of Co and Fe in β-Zr and β-Zr-alloys, Mater. Sci. Forum 15–18 (1987) p. 481.